Supplemental Information

Local spring effect in titanium-based layered oxides

Heng Su[ab,1], Gencai Guo[a,1], Yang Ren[c], Xiqian Yu[d], Xu Zhang[a], Tianyuan Ma[b], Yue Lu[e], Zihe Zhang[a], Hao Ma[a], Manling Sui[e], Hong Li[d], Chengjun Sun[c], Zonghai Chen[b], Guiliang Xu[b], Ruzhi Wang[a], Khalil Amine[bfg]* and Haijun Yu[a]**

[a]Faculty of Materials and Manufacturing, Key Laboratory of Advanced Functional Materials, Education Ministry of China, Beijing University of Technology, Beijing 100124, P.R. China; Email: hj-yu@bjut.edu.cn.

[b]Chemical Sciences and Engineering Division, Argonne National Laboratory, Argonne, Illinois 60439, USA.

[c]X-ray Science Division, Argonne National Laboratory, 9700 South Cass Avenue, Argonne, IL 60439 (USA).

[d]Key Laboratory for Renewable Energy, Beijing Key Laboratory for New Energy Materials and Devices, National Laboratory for Condensed Matter Physics, Institute of Physics, Chinese academy of Sciences, Beijing, 100190, China.

[e]Institute of Solid State Microstructure and Properties, Beijing University of Technology, Pingleyuan #100, Chaoyang District, Beijing 100124, China.

[f]Department of Material Science and Engineering, Stanford University, Stanford, CA 94305, USA.

[g]Institute for Research and Medical Consultations (IRMC), Imam Abdulrahman Bin Faisal University (IAU), Dammam, 34212 Saudi Arabia.

[1]These authors contributed equally to this work.

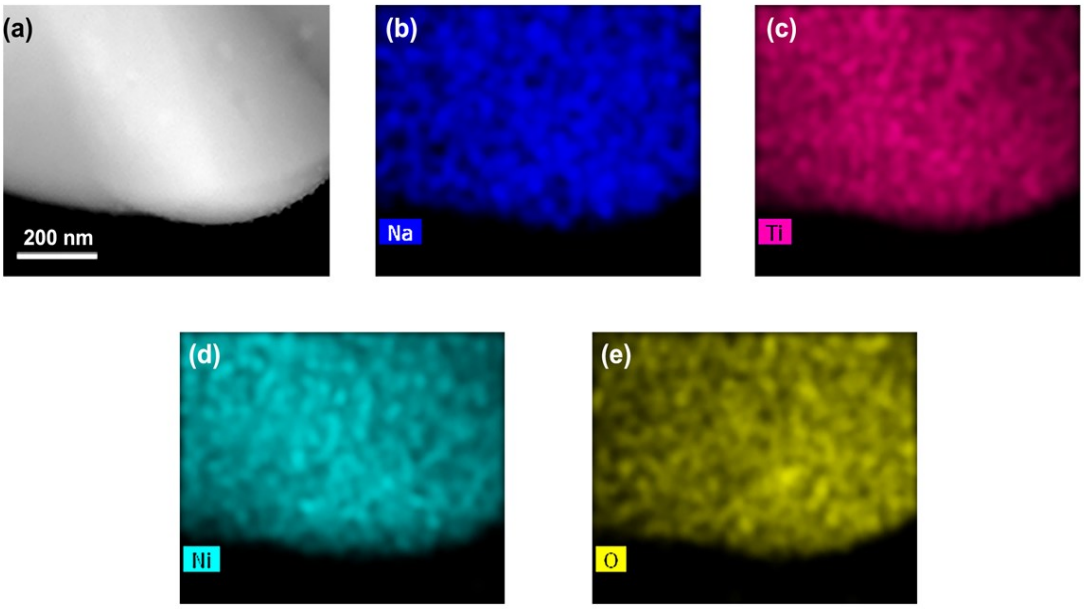

Fig. S1. (a) High-angle annular dark-field (HAADF) TEM image of the pristine P2-NNT. (b-e) The corresponding elemental maps including Na (b), Ti (c), Ni (d), and O (e).

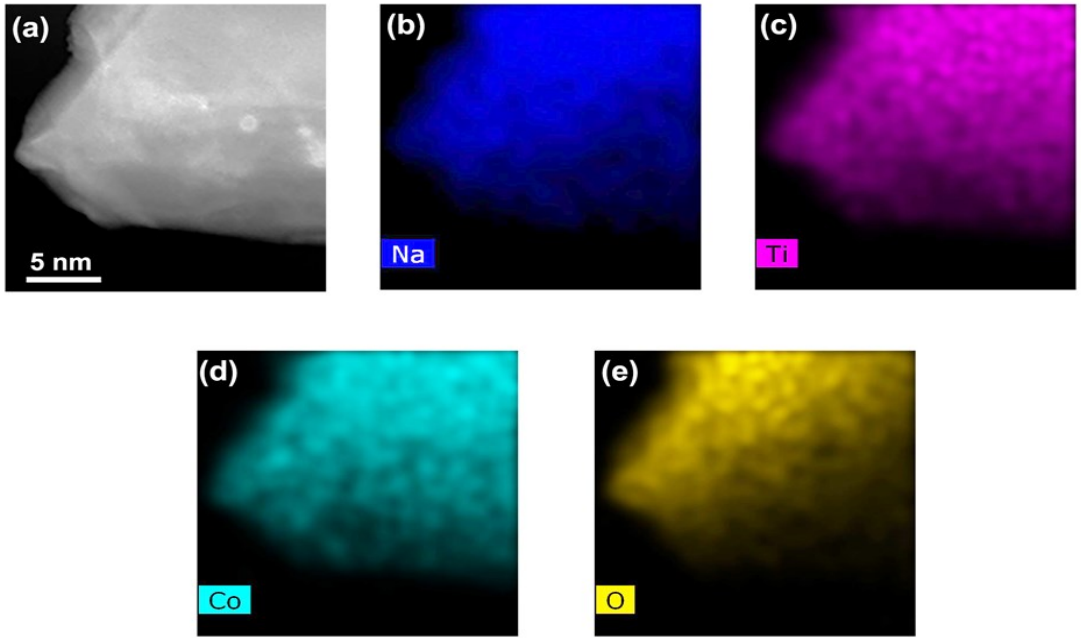

Fig. S2. (a) High-angle annular dark-field (HAADF) TEM image of the pristine P2-NCT. (b-e) The corresponding elemental maps including Na (b), Ti (c), Ni (d), and O (e).

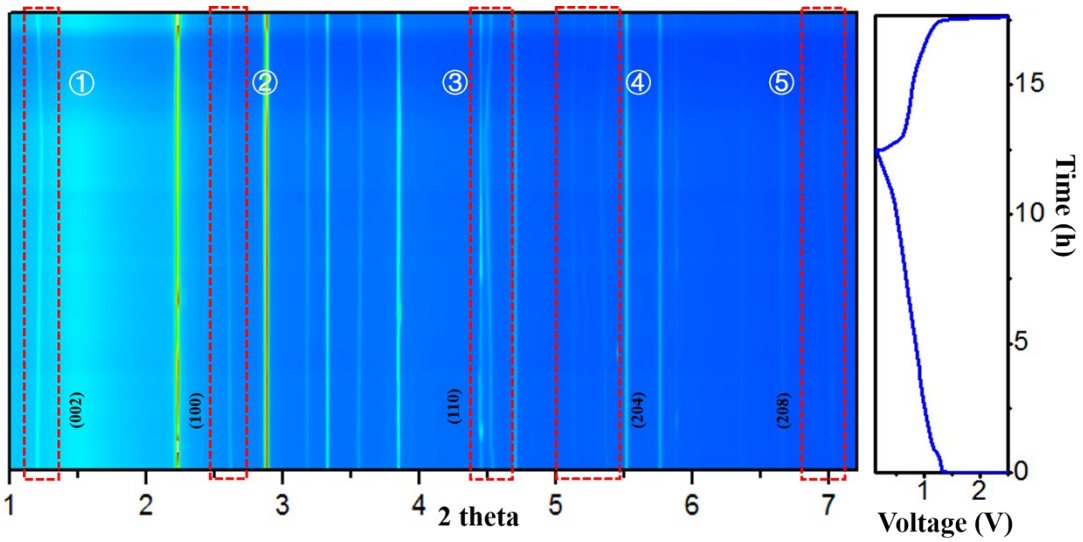

Fig. S3. HEXRD patterns of P2-NCT. The red rectangles labeled ①, ②, ③, ④ and ⑤ correspond to the regions of (002), (100), (110), (204), and (208) peaks, respectively. All the peaks can be indexed into a pure P2-type structure and smoothly shift without any new peak generation, indicating a solid solution mechanism. The right part of Fig. S3 shows the discharge/charge curves of P2-NCT in the first cycle at 0.1 C between 0-2.5 V.

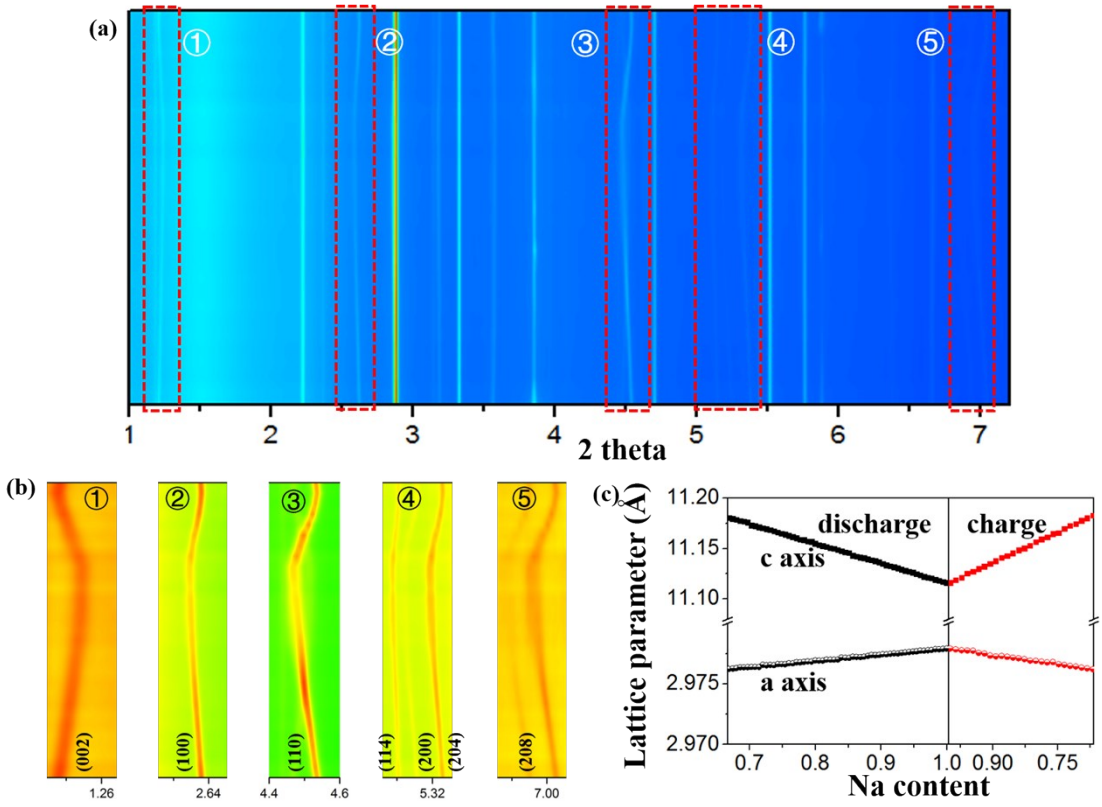

Fig. S4. *In-situ* HEXRD of P2-NNT in the second cycle. The red rectangles labeled ①, ②, ③, ④ and ⑤ correspond to the regions of (002), (100), (110), (204), and (208) peaks, respectively. (a) Patterns collected during the second cycle between 0.15-2.5 V at 0.1C. (b) Enlarged *In-situ* HEXRD patterns of the red dash-line rectangles in Fig. S4a. (c) The evolution of lattice parameters *a* and *c* during the charge and discharge process. All the peaks can be indexed into a pure P2-type structure and smoothly shift without any new peak generation, indicating a solid solution mechanism.

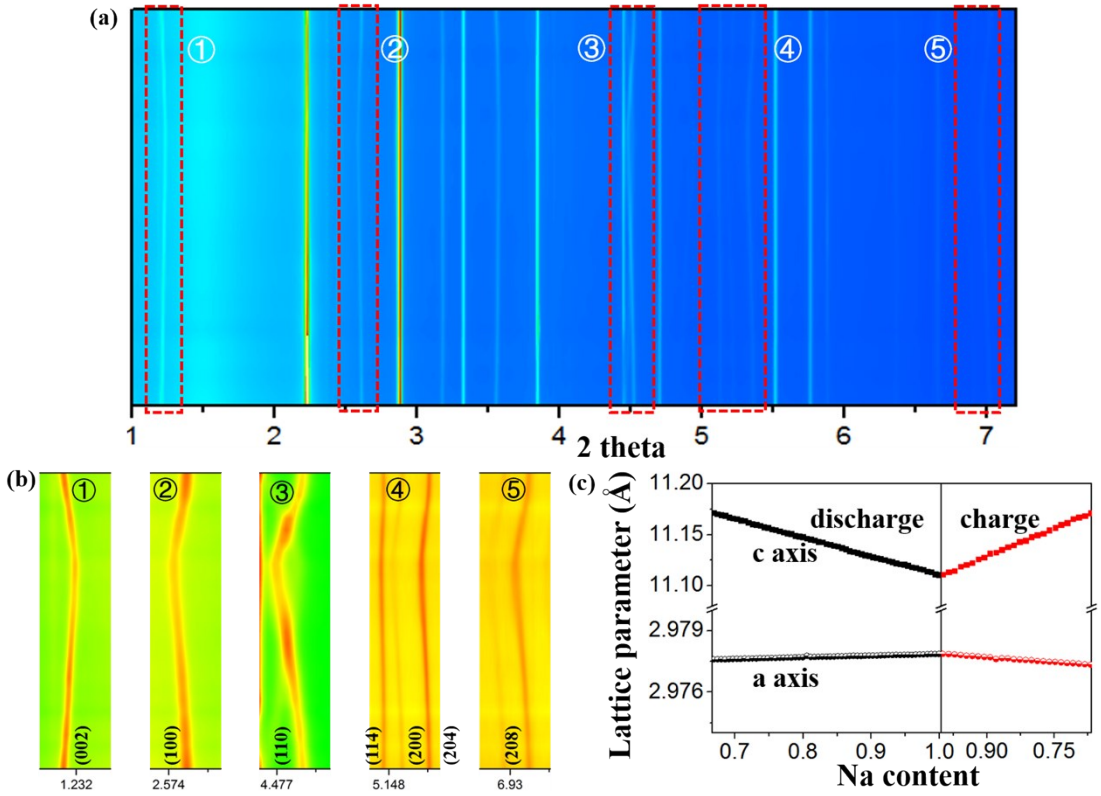

Fig. S5. *In-situ* HEXRD of P2-NCT in the second cycle. The red rectangles labeled ①, ②, ③, ④ and ⑤ correspond to the regions of (002), (100), (110), (204), and (208) peaks, respectively. (a) Patterns collected during the second cycle between 0.15-2.5 V at 0.1C. (b) Enlarged *In-situ* HEXRD patterns of the red dash-line rectangles in Fig. S5a. (c) The evolution of lattice parameters *a* and *c* during the charge and discharge process. All the peaks can be indexed into a pure P2-type structure and smoothly shift without any new peak generation, indicating a solid solution mechanism.

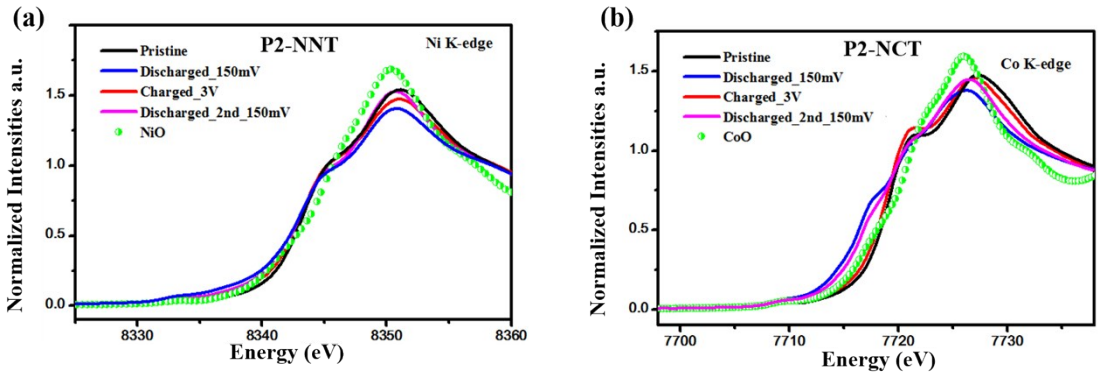

Fig. S6. *Ex-situ* Ni K-edge XANES spectra of P2-NNT (a) and Co K-edge XANES spectra of P2-NCT at the pristine, fully charged, and fully discharged states.

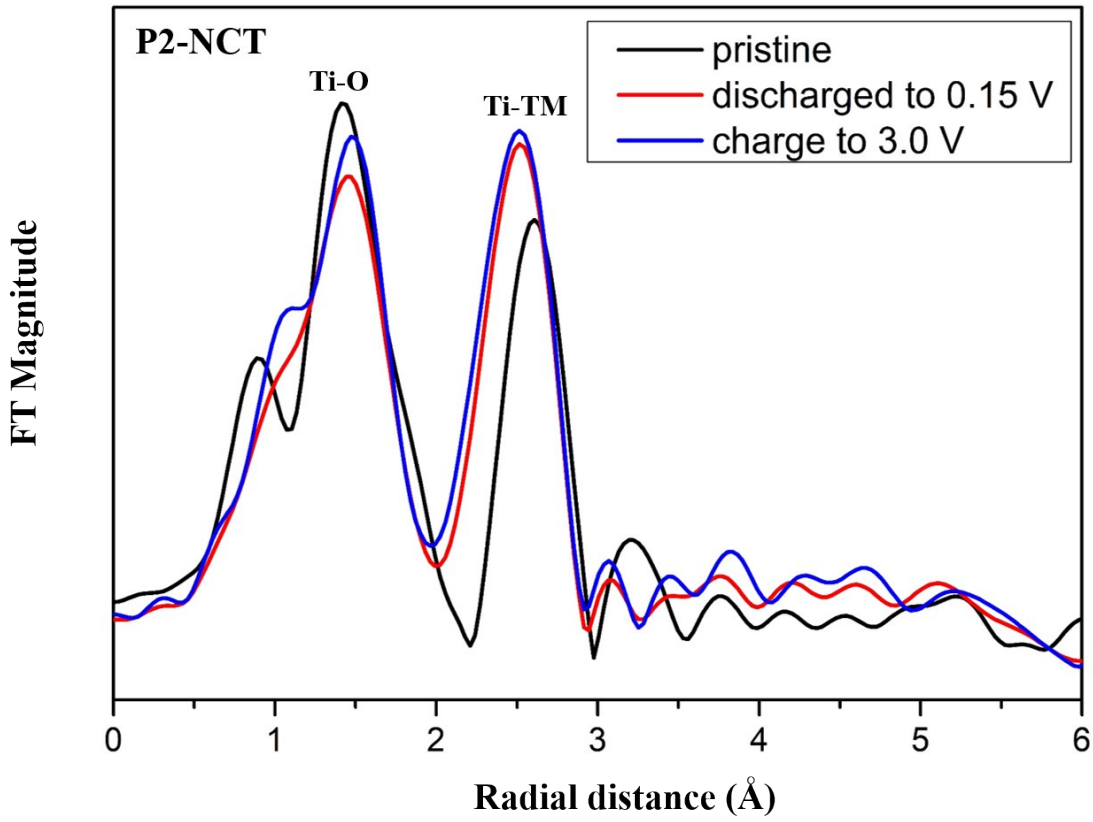

Fig. S7. Fourier transform data of Ti K-edge XANES spectra of the P2-NCT electrode at the pristine (black line), discharged (red line), and charged states (blue line).

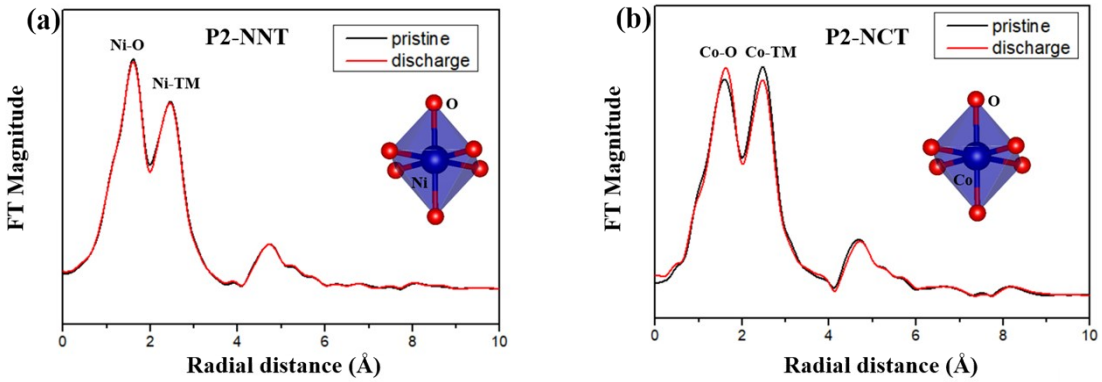

Fig. S8. Fourier transform data of (a) Ni K-edge XANES spectra of P2-NNT electrode and (b) Co K-edge XANES spectra of P2-NCT electrode at the pristine (blue line) and discharged states (red line).

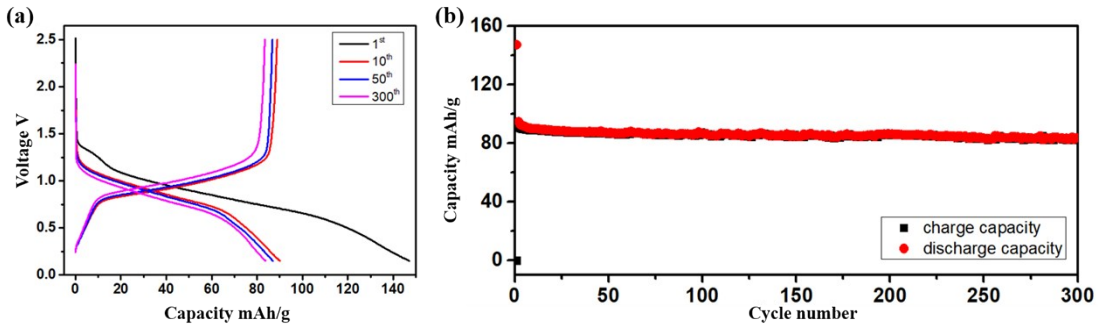

Fig. S9. (a) Charge/discharge profiles of of P2-NNT in the 1st, 10th, 50th and 300th cycles and (b) the long-cycle performance at 0.2 C.

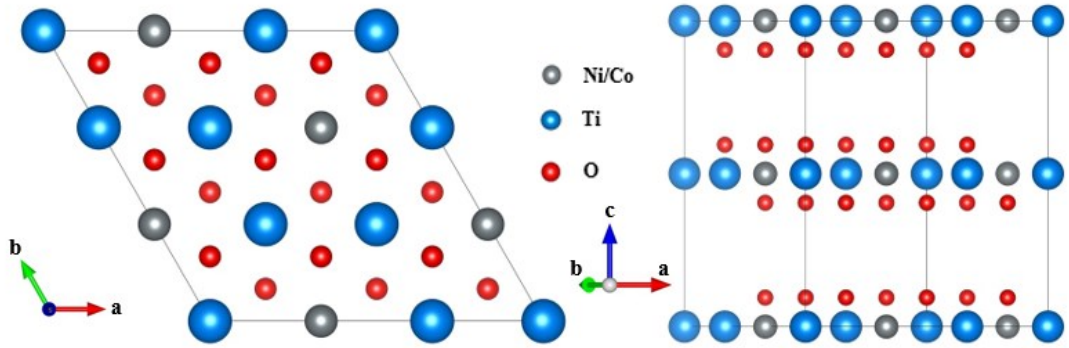

Fig. S10. The first possible TM arrangement in P2-type structure. The same TM ions are over against each other in this model.

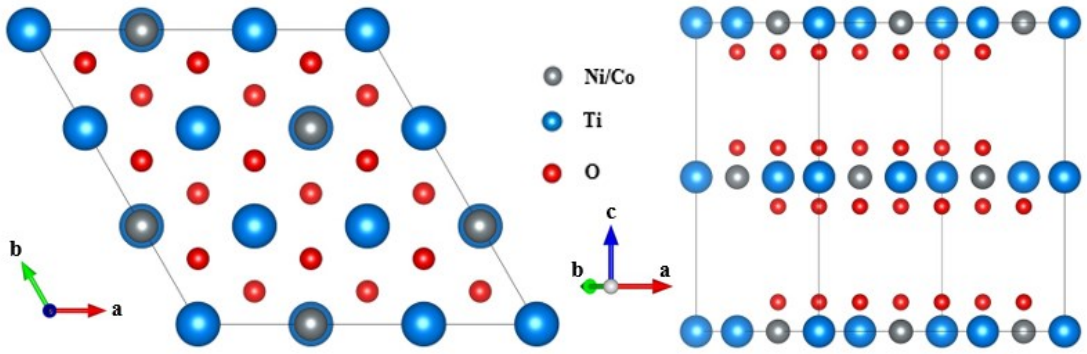

Fig. S11. The second possible TM arrangement in P2-type structure. Ni/Co and Ti ions are alternately located in different layers with each other.

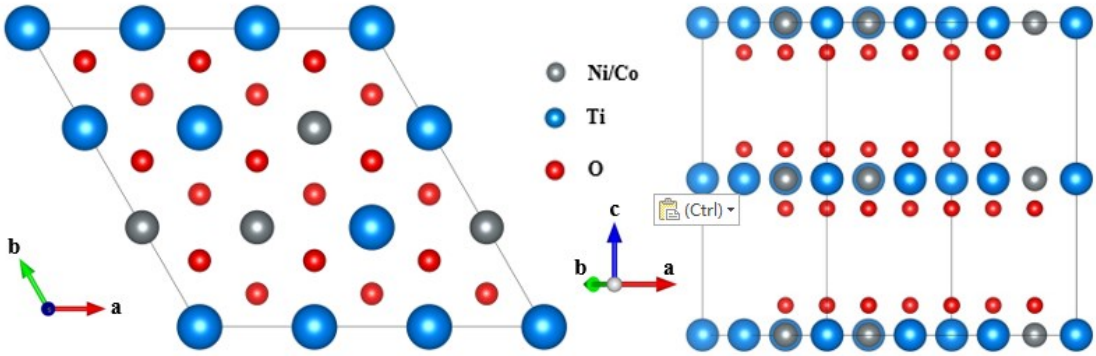

Fig. S12. The third possible TM arrangement in P2-type structure. Ni/Co ions and Ti ions are alternately located with each other in this model.

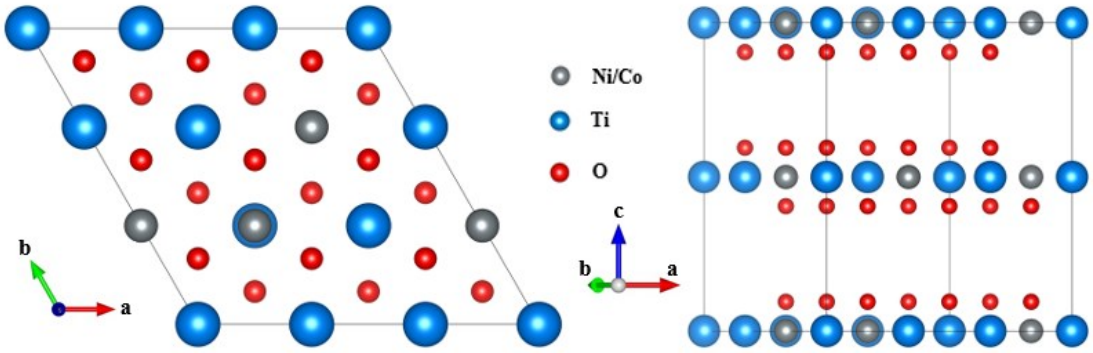

Fig. S13. The fourth possible TM arrangement in P2-type structure. Ni/Co and Ti ions are alternately located with each other in the same layers, and the same TM ions are over against each other in this model.

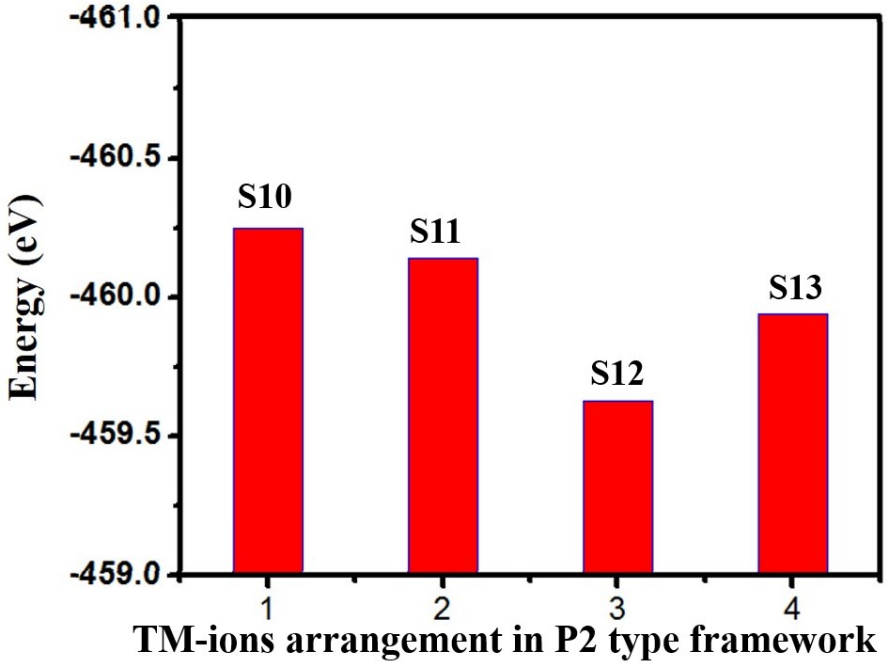

Fig. S14. The total energies of the four models in Fig. S10-S13. The structure model in Fig. S10 has the lowest formation energy, indicating its highest stability among all structures.

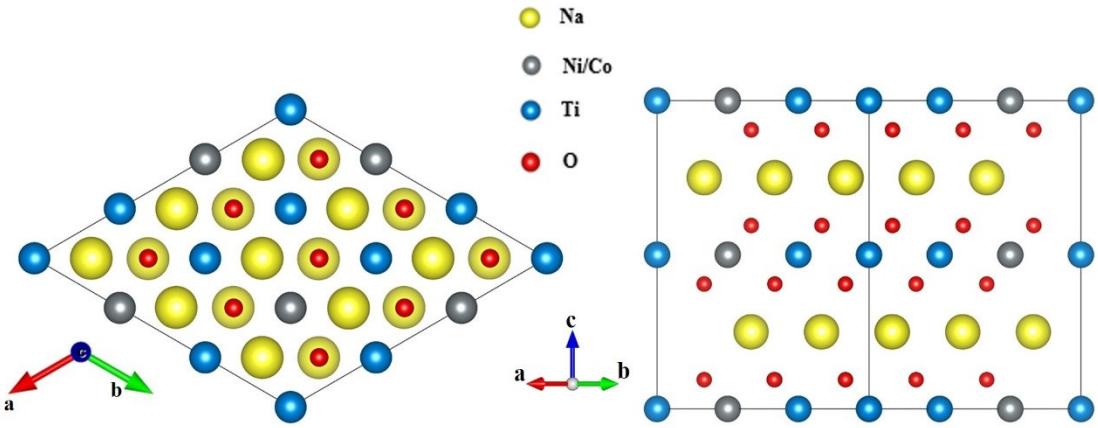

Fig. S15. The first possible Na^+ arrangement in P2-type structure. All the Na^+ ions are located in Na_e sites in this model.

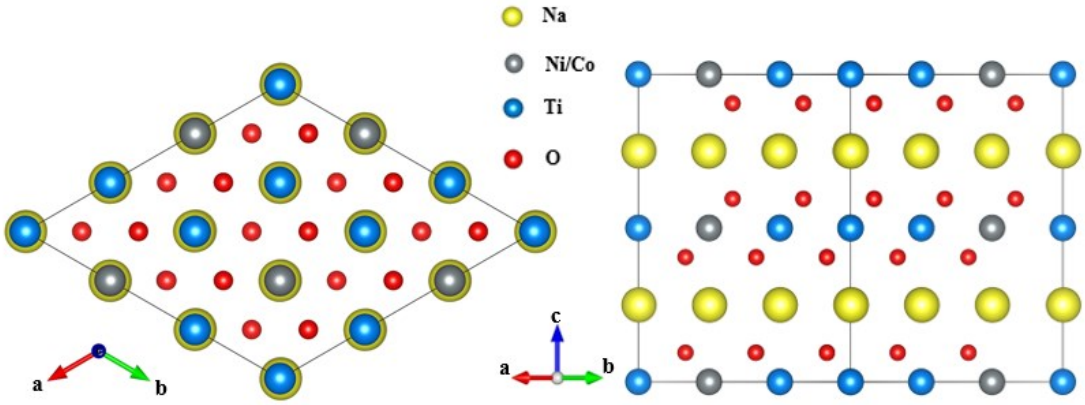

Fig. S16. The second possible Na^+ arrangement in P2-type structure. All the Na^+ are located in Na_f sites in this model.

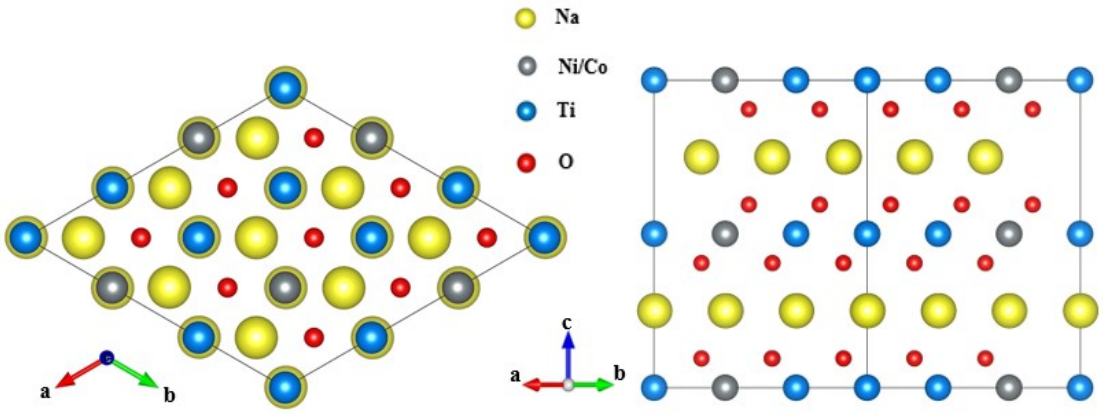

Fig. S17. The third possible Na^+ arrangement in P2-type structure. Na^+ ions are located in Na_e and Na_f sites with a ratio of 2:1 in this model.

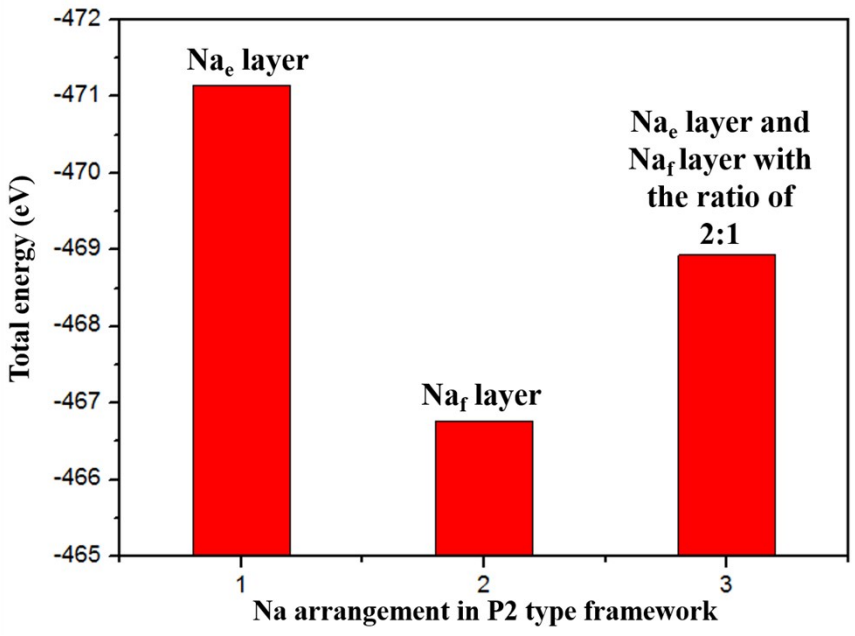

Fig. S18. The total energies of the three models in Fig. S15-S17. The structure model with only Na_e layers has the lowest formation energy, indicating its highest stability among all models.

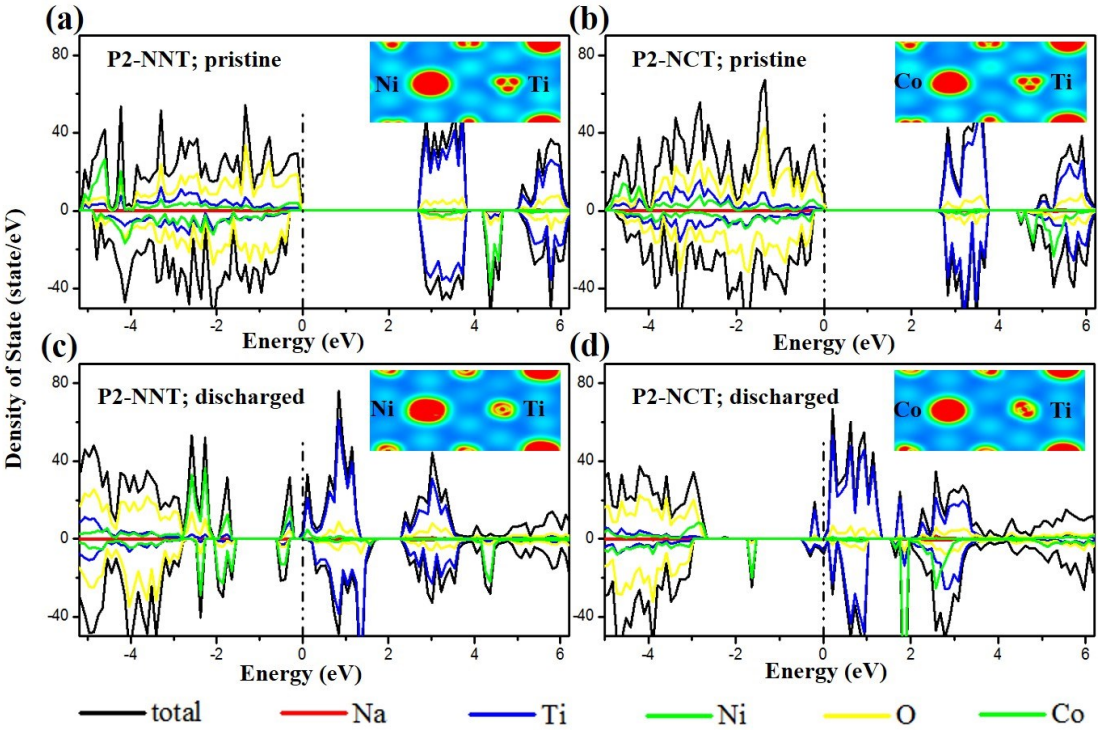

Fig. S19. The projected density of state (DOS) of (a) pristine state of P2-NNT, (b) pristine state of P2-NCT, (c) fully discharged state of P2-NNT, and (d) fully discharged state of P2-NCT. Insets in a-d are the corresponding charge density distribution images. The DOS values of total, Na, Ti, Ni/Co, and O are shown in black, red, blue, green and yellow lines, respectively.

Table S1. Rietveld refinement results of P2-NNT with lattice parameters *a* and *c*.

Rwp: 5.161; Rexp: 2.57; GOF: 2.01				space group: P63/mmc (194)	
Lattice Parameter	a		c		
	2.96482(7)		11.1669(6)		
atom	**x**	**y**	**z**	**Occ.**	**Beq.**
Na-1	0.33333	0.66667	0.25000	0.455(4)	2.88
Na-2	0.00000	0.00000	0.25000	0.214(6)	4.2
Ti	0.00000	0.00000	0.00000	0.666(4)	0.6
Ni	0.00000	0.00000	0.00000	0.334(2)	0.6
O	0.66667	0.33333	0.0941(2)	0.945(4)	0.9

Table S2. Rietveld refinement results of P2-NCT with lattice parameters *a* and *c*.

Rwp: 4.574; Rexp: 3.23; GOF: 1.41			space group: P63/mmc (194)		
Lattice Parameter	a		c		
	2.97262(6)		11.1929(7)		
atom	**x**	**y**	**z**	**Occ.**	**Beq.**
Na-1	0.33333	0.66667	0.25000	0.461(8)	2.88
Na-2	0.00000	0.00000	0.25000	0.218(6)	4.2
Ti	0.00000	0.00000	0.00000	0.662(3)	0.6
Co	0.00000	0.00000	0.00000	0.338(5)	0.6
O	0.66667	0.33333	0.0923(8)	0.979(8)	0.9